J. Inverse Ill-Posed Probl. **22** (2014), 609–623
DOI 10.1515/jip-2013-0060

Acoustic impedance inversion with covariation approach

Bi B. Yue and Zhen M. Peng

Abstract. This paper presents a novel covariation approach for seismic inversion under the assumption that the real seismic signals follow non-Gaussian α-stable distribution. To verify the correctness and effectiveness of the proposed method, two computer inversion simulation experiments on synthetic data inversion and real seismic acoustic impedance inversion are conducted using covariation, covariance and Bayesian methods. In the inversion experiment, covariation method performances better than the covariance and Bayesian, and the inverse results are very close to the true solutions. In the real seismic data inversion case, the sample quantile method was applied to estimate the characteristic exponent of a seismic trace from a nearby well before inversion. The estimated characteristic was applied in the 2D seismic impedance inversion where the moment p of the whole survey is set to be less than it. The results from the inversion of the 2D real data set are consistent with the well log interpretation.

Keywords. Fractional lower order moment, covariation, α-stable distribution, non-Gaussian, acoustic impedance inversion.

2010 Mathematics Subject Classification. 11Y16, 15A09, 15A29, 15A90.

1 Introduction

Seismic acoustic impedance inversion is an important technique to reconstruct acoustic impedance profile of the Earth. Standard seismic acoustic inversion techniques assume that the seismic signals follow Gaussian distribution, based on which a great deal of estimation methods have been proposed (e.g. Srivastava–Sen [13], Yang–Song–Hao [18] and Yue–Peng–Hong–Zou [19]). However, in the recent years, non-Gaussian seismic inversion techniques are attracting considerable attention and many non-Gaussian distribution seismic signal models are proposed, for example, Walden [15] modeled the reflection coefficient amplitude distribution by generalized Gaussian, Godfrey–Claerbout [4] chose the generalized Cauchy distribution as empirical distribution about the reflection coefficient.

This work was supported by National Natural Science Foundation of China Grants No. 41274127, 40874066, 40839905 and the Fundamental Research Funds for the Central Universities Grant No. ZYGX2011YB021.

Yue–Peng–Zhang [20] studied the heavy tailed character of seismic signals and proposed that seismic signal follows non-Gaussian $\boldsymbol{\alpha}$-stable distribution.

In this paper, non-Gaussian $\boldsymbol{\alpha}$-stable distribution is taken as the statistical distribution of seismic data. The non-Gaussian $\boldsymbol{\alpha}$-stable distributions have algebraic tail which is significantly thicker than that of Gaussian distribution (see Liu–Mendel [7], Shao–Nikias [12], Nikias–Shao [11], Tsaklides–Nikiaas [14] and Liu–Wang–Qiu [8]). A consequence of thicker tails of $\boldsymbol{\alpha}$-stable distributions is that there is non-existence of the second or higher order moments of $\boldsymbol{\alpha}$-stable distributions, only moments of order less than α are finite, except for the limiting case $\alpha = 2$. However, for non-Gaussian $\boldsymbol{\alpha}$-stable distributions, the fractional lower order statistics do exist (see Gao–Qiu–Zhang [3] and Conti–Roisenberg–Neto–Posani [1]). A quantity called covariation (see Wang–Zhu [17], Leite–Vidal [6], Ma–Nikias [9], Wang–Kuruoglu–Zhou [16]) is applied in the seismic inversion process. The role of covariation function for an $\boldsymbol{\alpha}$-stable distribution is analogous to the role of covariance function for Gaussian signal.

The rest of the paper is organized as follows: In Section 2, some necessary preliminaries on $\boldsymbol{\alpha}$-stable distribution and covariation are presented. In Section 3, seismic estimation by using covariation approach is formulated and synthetic data inversion experiment is conducted to test the performance of the covariation inversion method. In Section 4, real seismic acoustic impedance inversion is conducted, the results verify the correctness and effectiveness of the proposed wavelet estimation. Finally, the discussions and conclusions drawn from the inversion results are covered in Section 5.

2 α-stable distributions and covariation

Unlike most statistical models, the $\boldsymbol{\alpha}$-stable distributions do not have close form probability density functions except for a few known cases. The characteristic function of the $\boldsymbol{\alpha}$-stable distributions (see Liu–Mendel [7], Shao–Nikias [12] and Nikias–Shao [11]) is

$$\varphi(u) = \exp\{j\mu u - \gamma|u|^{\alpha}[1 + j\beta \operatorname{sgn}(u) w(u,\alpha)]\}, \tag{2.1}$$

where

$$w(u,\alpha) = \begin{cases} \tan(\frac{\pi\alpha}{2}), & \alpha \neq 0, \\ \frac{2}{\pi}\log(u), & \alpha = 0, \end{cases} \tag{2.2}$$

$$\operatorname{sgn}(u) = \begin{cases} 1, & u > 0, \\ 0, & u = 0, \\ -1, & u < 0. \end{cases} \tag{2.3}$$

The stable characteristic function is completely determined by four parameters: α $(0 < \alpha \leq 2)$ the characteristic exponent, β $(-1 \leq \beta \leq 1)$ the symmetry parameter, γ $(\gamma > 0)$ the dispersion, and the location parameter. When $\beta = 0$, the $\boldsymbol{\alpha}$-stable distribution is called symmetry $\boldsymbol{\alpha}$-stable $(S\alpha S)$ distribution.

For jointly $S\alpha S$ distribution variables X and Y with $1 < \alpha < 2$, the covariation of them is defined as (Tsaklides–Nikias [14], Liu–Wang–Qiu [8], Gao–Qiu–Zhang [3])

$$[X, Y]_\alpha = \frac{E(XY^{\langle p-1 \rangle})}{E(|Y|^p)} \gamma_Y, \quad 1 \leq p < \alpha, \tag{2.4}$$

where γ_Y is the dispersion of Y. According to equation (2.4), one has

$$\gamma_Y = [Y, Y]_\alpha. \tag{2.5}$$

The covariation coefficient of X with Y is defined by

$$\lambda_{X,Y} = \frac{[X, Y]_\alpha}{[Y, Y]_\alpha}. \tag{2.6}$$

Combining equations (2.4), (2.5) and (2.6), the covariation coefficient $\lambda_{X,Y}$ is also defined as

$$\lambda_{X,Y} = \frac{E(XY^{\langle p-1 \rangle})}{E(|Y|^p)}, \quad 1 \leq p < \alpha, \tag{2.7}$$

Below, some important properties of covariations (see Shao–Nikias [12]) are listed that are later used in Section 4 of the paper:

(1) The covariation $[X, Y]_\alpha$ is linear in X. If X_1, X_2 and Y are jointly $S\alpha S$, then

$$[AX_1 + BX_2, Y]_\alpha = A[X_1, Y]_\alpha + B[X_2, Y]_\alpha \tag{2.8}$$

for any real constants A and B.

(2) The covariation $[X, Y]_\alpha$ is pseudo-linear in Y. If Y_1, Y_2 and X are independent and jointly $S\alpha S$, then

$$[X, AY_1 + BY_2]_\alpha = A^{\langle \alpha-1 \rangle}[X, Y_1]_\alpha + B^{\langle \alpha-1 \rangle}[X, Y_2]_\alpha \tag{2.9}$$

for any real constants A and B.

(3) If X and Y are independent, then

$$[X, Y]_\alpha = 0. \tag{2.10}$$

For $n+1$ jointly non-Gaussian $S\alpha S$ random variables $X_0, X_1, \dots, X_n$ with $1 < \alpha < 2$, the regression of X_0 in terms of $X_1, \dots, X_n$ is the conditional expectation $E(X_0 \mid X_1, \dots, X_n)$. In the non-Gaussian $S\alpha S$ case, the conditional expectation is not linear in general, unless certain conditions are satisfied. Suppose that the random variables $X_1, \dots, X_n$ are independent and non-degenerate. Then

$$E(X_0 \mid X_1, \dots, X_n) = \lambda_{01} X_1 + \dots + \lambda_{0n} X_n, \tag{2.11}$$

where λ_{0i} is the covariation coefficient of X_0 and X_i, $i = 1, \dots, n$.

In particular, for any two jointly $S\alpha S$ random variables X and Y, we get

$$E(X \mid Y) = \lambda_{XY} Y. \tag{2.12}$$

3 Acoustic impedance inversion with covariation

Seismic inversion methods are generally based on the convolution model that treats a seismic trace $s = [s(1), s(2), \dots, s(N)]^T$ as the convolution of the seismic wavelet $w = [w(1), w(2), \dots, w(K)]^T$ and the Earth's reflection coefficient serial $r = [r(1), r(2), \dots, r(M)]^T$ and the addition of this convolution with a random noise $U = [u(1), u(2), \dots, u(N)]^T$. So the seismic signal can be modeled by means of the following equation (Conti–Roisenberg–Neto–Posani [1]):

$$s = w * r + U, \tag{3.1}$$

where '$*$' represents the convolution operation and the addition noise is modeled as $S\alpha S$ random noise, the lengths of data satisfy $N = M + K - 1$.

According to the convolution rule, the Earth is modeled as a linear system represented by reflection coefficient r, and the seismic trace s is the result of the input source wavelet w acting on the Earth system. Figure 1 illustrates the process of generating a seismic trace. The sample $s(n)$ $(n = 1, 2, \dots, N)$ in formula (3.1) is given by the following equation (Wang–Zhu [17]):

$$\begin{aligned} s(n) &= \sum_{i=1}^{n} r(j) w(n-j+1) + U(n) \\ &= r(1)w(n) + r(2)w(n-1) + \dots + r(M)w(n-M+1) + U(n). \end{aligned} \tag{3.2}$$

In this paper, the assumption that the seismic signals are $S\alpha S$ is believed because they have no finite variance, and covariation method is applied to seismic inversion. The covariation of seismic trace $s(n)$ and wavelet $w(n)$ is defined as

$$\begin{aligned} R_{s,w}(m) &= E\{s(n)[w(n+m)]^{\langle p-1 \rangle}\} \\ &= E\{s(n)|w(n+m)|^{p-1} \operatorname{sgn}[w(n+m)]\}, \end{aligned} \tag{3.3}$$

Figure 1. Block diagram of seismic trace generating.

where $1 \leq p < \alpha$. Generally, the covariation is estimated by the sample covariation

$$\hat{R}_{s,w}(m) = \frac{1}{N} \sum_{n=1}^{N} s(n)|w(n+m)|^{p-1} \operatorname{sgn}[w(n+m)]. \tag{3.4}$$

According to equation (3.4), we obtain the following expression for the covariation of the seismic trace s and the wavelet w:

$$E[s(i)w(l)^{\langle p-1\rangle}] = E\left[\left(\sum_{j=1}^{M} r(i,j)w(j)\right) w(l)^{\langle p-1\rangle}\right]. \tag{3.5}$$

Combining equations (3.4) and (3.5), we can obtain the following expression:

$$\Gamma_{sw} = \Gamma_w r, \tag{3.6}$$

where $\Gamma_{sw} = [R_{s,w}(1), R_{s,w}(2), \ldots, R_{s,w}(M)]^T$ is the covariation array of the seismic data s and the wavelet w, $r = [r(1), r(2), \ldots, r(M)]^T$ is the reflection coefficient, and the wavelet covariation matrix is

$$\Gamma_w = \begin{pmatrix} R_{w,w}(0) & R_{w,w}(-1) & \cdots & R_{w,w}(1-M) \\ R_{w,w}(1) & R_{w,w}(0) & \cdots & R_{w,w}(2-M) \\ \vdots & & \ddots & \vdots \\ R_{w,w}(M-1) & R_{w,w}(M-2) & \cdots & R_{w,w}(0) \end{pmatrix}.$$

Clearly, when $p = 2$, i.e., for Gaussian distributed signals, the expression for the covariation matrix is reduced to the well-known form of the covariance matrix. Hence, the source wavelet vector can be obtained from equation (3.6) with inversion techniques such as singular value decomposition algorithm.

However, the input wavelet w, a representation of the explosive seismic source signal, is always much shorter than seismic trace. In many real seismic inversion applications, for example, the length of the wavelet is set about 100 ms, while the length of seismic data between the inversion layers may be more than 300 ms. For this reason, the wavelet was padded with zeros such that it is consistent with the length of seismic trace.

4 Acoustic impedance inversion

4.1 Impedance inversion with covariation

Impedance contains important information concerning the nature of the rock and changes in lithology. Although there are many forms of impedances, for example, acoustic impedance, elastic impedance and extended elastic impedance, a similar inversion process is used to estimate the impedance values. The inversion method proposed in this paper can also be used to estimate impedance values.

It is well known that the reflection coefficient r is directly related to the contrast in the impedance Z of superposed layers through the expression (Leite–Vidal [6])

$$r_i = \frac{Z_{i+1} - Z_i}{Z_{i+1} + Z_i}, \tag{4.1}$$

where Z_i is impedance in the ith layer, and r_i is the reflection coefficient at the ith interface of a set of $M + 1$ superposed layers.

According to equation (4.1), the impedance Z_{i+1}-value of $(i + 1)$th layer can be calculated from the knowledge of the Z_i-value of the ith layer through a recursive equation

$$Z_{i+1} = Z_i \frac{1 + r_i}{1 - r_i}, \tag{4.2}$$

which in turn can be generalized to provide the impedance value of a arbitrary layer by

$$Z_j = Z_0 \prod_{i=1}^{j-1} \frac{1 + r_i}{1 - r_i}. \tag{4.3}$$

The nature logarithm is applied to both sides of equation (4.3) and one will get

$$\ln(Z_j) = \ln(Z_0) + \sum_{i=1}^{j-1} 2(r_i + \frac{r_i^3}{3}) + \frac{r_i^5}{5} + \cdots. \tag{4.4}$$

Discarding the high order terms of equation (4.4), it leads to the expression

$$\ln(Z_j) - \ln(Z_0) = 2 \sum_{i=1}^{j-1} r_i. \tag{4.5}$$

If we set $L_i = \ln(Z_i)$, one can rewrite (4.5) in matrix form as

$$\begin{pmatrix} r_1 \\ r_2 \\ \vdots \\ r_M \end{pmatrix} = \begin{pmatrix} -\frac{1}{2} & \frac{1}{2} & 0 & \cdots & 0 \\ 0 & -\frac{1}{2} & \frac{1}{2} & \cdots & 0 \\ \vdots & \ddots & & & \vdots \\ 0 & 0 & 0 & \cdots & \frac{1}{2} \end{pmatrix} \begin{pmatrix} L_0 \\ L_2 \\ \vdots \\ L_M \end{pmatrix} \tag{4.6}$$

or

$$r = DL \tag{4.7}$$

where $L = (L_0, L_2, \dots, L_M)^T = (\ln(Z_0), \ln(Z_1), \dots, \ln(Z_M))^T$.

Therefore, (3.6) can be rewritten as

$$\Gamma_{sw} = \Gamma_w DL = AL, \tag{4.8}$$

where $A = \Gamma_w D$ is a substitute matrix, other variables are the same as those in equation (3.6).

4.2 Characteristic estimation

It is known that, for non-Gaussian $\boldsymbol{\alpha}$-stable distributions, only moments of characteristic less than α are finite. In particular, the second order moment of an $\boldsymbol{\alpha}$-stable distribution with $\alpha < 2$ does not exist.

In our proposed method, characteristic α plays a key role in moment choosing. However, the estimation of non-Gaussian $\boldsymbol{\alpha}$-stable distributions is general severely hampered by the lack of known closed form density functions (see Ma–Nikias [9] and Wang–Kuruoglu–Zhou [16]). There is a useful suboptimal numerical method named sample quantile method (Fame–Roll [2]) applied to estimate the characteristic α, McCulloch [10] generalized and improved their method. He analyzed stable law quantiles and provided consistent estimators of all four stable parameters, with the restriction $\alpha > 0.6$ while retaining the computational simplicity of Fame–Roll's method. It is a simple and frequently way for roughly estimating the parameters of an $S\alpha S$ distribution with $1 \le \alpha < 2$.

In this approach, the following definition is used:

$$v_\alpha = \frac{x_{0.95} - x_{0.05}}{x_{0.75} - x_{0.25}}.$$

In the above formula x_f denotes the fth population quantile, so that $f = F(x_f)$, where $F(x_f)$ is a distribution function, roughly estimated by a histogram of data in this paper. For $S\alpha S$, $\beta = 0$. An estimate, $\hat{\alpha}$, can be obtained by searching a table of standard distribution functions. Table 1 is derived from McCulloch's tabulation [10].

v_α	2.439	2.5	2.6	2.7	2.8	3.0	3.2	3.5	4.0	5.0	6.0
α	2.000	1.916	1.808	1.729	1.664	1.563	1.484	1.391	1.279	1.128	1.029

Table 1. Values of v_α and α.

4.3 Synthetic data inversion

The proposed covariation method is applied in the following synthetic data inversion, and the data are shown in Figure 2. Figure 2 (a) is the reflection coefficient composed of several spikes, Figure 2 (b) is the Ricker wavelet with center frequency 40 Hz, Figure 2 (c) is the extended Ricker wavelet with zeros, and Figure 2 (d) is the synthetic seismic trace convoluted by the reflection coefficient and Ricker wavelet. As the reflection coefficient has strong spike characteristic, the moment of covariation was set $p = 1.2$. In order to evaluate the performance of the covariation inversion method, we compare its result with the traditional covariance method and Bayesian seismic inversion method applied by Gunning–Glinskey [5].

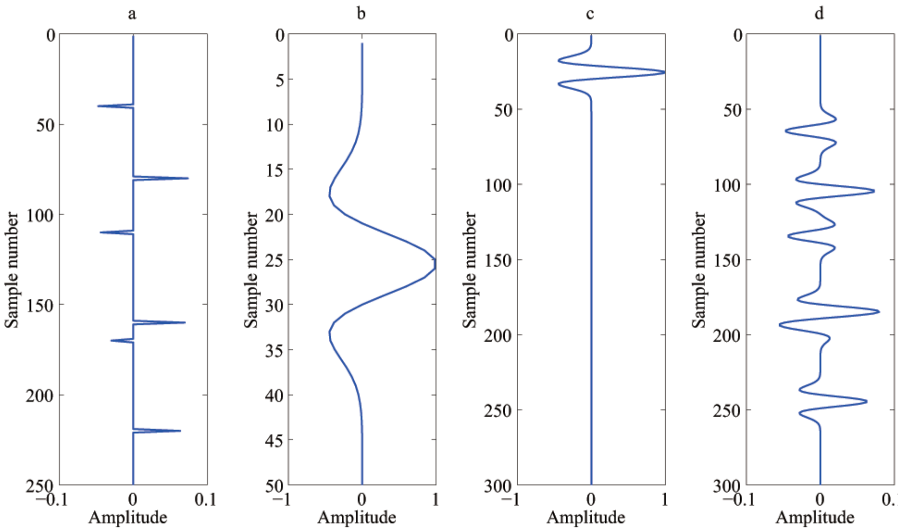

Figure 2. Synthetic data: (a) reflection coefficient, (b) Ricker wavelet, (c) extended Ricker wavelet, (d) synthetic seismic trace.

The inversion results are shown in Figure 3, where Figure 3 (a) is the inversion result of the covariance method, Figure 3 (b) is the result of the Bayesian method and Figure 3 (b) is the result of the covariation method. As shown in the figure, all of the three methods obtain the results are approximately consistent with true reflection. However, the covariation method performs better than the covariance and Bayesian, especially, where the value of true reflection is 0, marked with arrows in Figure 3, the covariation method gets more precise than the others.

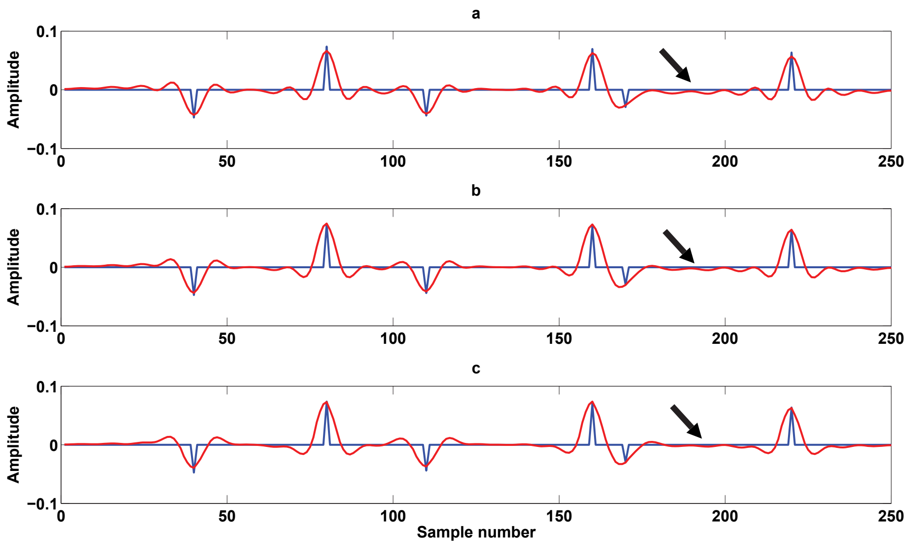

Figure 3. Inversion result: (a) inversion result of the covariance method, (b) inversion result of the Bayesian method, (c) inversion result of the covariation method.

4.4 Real data inversion

In this subsection, we demonstrate an application of our method to the real seismic data. The seismic data used in this study were collected from a survey in the south of Sichuan, China, and CDP number of the only available well is 435.

Before performing the inversion, the seismic trace from a nearby well is used to estimating the characteristic α. We use the estimation method described in Section 4.2. The selected seismic trace and its histogram H are shown in Figure 4. When $f = \sum_{i=0}^{M} H(i)$, one has $x_i = S(M)$, where $S(1) \le S(2) \le \cdots \le S(N)$ is the ascending order of seismic trace. Based on this method, one obtains that $x_{0.95} = 2040.7$, $x_{0.75} = 681.7$, $x_{0.25} = -3395.7$ and $x_{0.05} = -8662.1$. Using the quantile method described in Section 4.2, one obtains $v_\alpha = 2.6250$. Searching in Table 1, the estimated characteristic of the seismic trace is $\hat{\alpha}_s = 1.7883$. Then the moment p of the whole survey must be less than $\hat{\alpha}_s$.

To verify the performance of the covariation inversion method, an experiment is conducted to estimate the acoustic impedance from a single seismic trace. The process used is similar to the approach applied to the synthetic data. In the experiment, a Ricker wavelet rather than a wavelet estimated from the real data is applied, to avoid the influence of wavelet residual. Figure 5 (a) is the acoustic impedance computed from the well, and the depth range of the impedance is between 4700 m and 5300 m. Figure 5 (b) is the reflection coefficient calculated

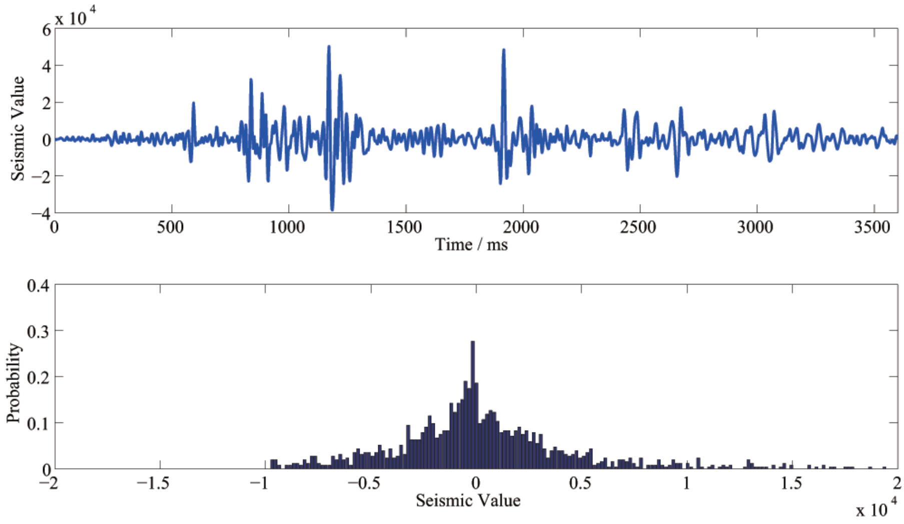

Figure 4. Seismic trace and its histogram.

using (4.1) above. Figure 5 (c) is the Ricker wavelet with center frequency 40 Hz. Figure 5 (d) is the synthetic seismic trace resulting from the convolution of the reflection coefficient and Ricker wavelet.

In this part, the inversion was conducted by the covariation, covariance and Bayesian methods. The covariation inversion was conducted using equation (4.8), and the moment of covariation is set $p = 1.6$. The inversion results are illustrated in Figure 6. The inversion results of the covariation, covariance and Bayesian methods are plotted in red, green and black, respectively. The impedance of the well is shown in blue. Although the three methods can obtain inversion results approximately consistent with true impedance, the covariation performs more precise than the covariance and Bayesian methods. Especially at pikes, marked with arrows in Figure 6, the covariation result is closer to the true impedance than the results of others.

To evaluate the covariation impedance inversion method, error analysis of covariation with $p = 1.6$ is conducted, as shown in Figure 7. The acoustic impedance from the well and the inversion result are shown in Figure 7 (a) and Figure 7 (b), respectively. It is clear that the acoustic impedance derived from the covariation inversion has a remarkable good agreement with the acoustic impedance from the well. The residual of impedance of the well and inverse result is shown in Figure 7 (c), that may be due to calculation error. To better compare the true and the estimated impedance values, the residual ratio (residual divided by original impedance) is defined. This is shown in Figure 7 (d) and provides a better view

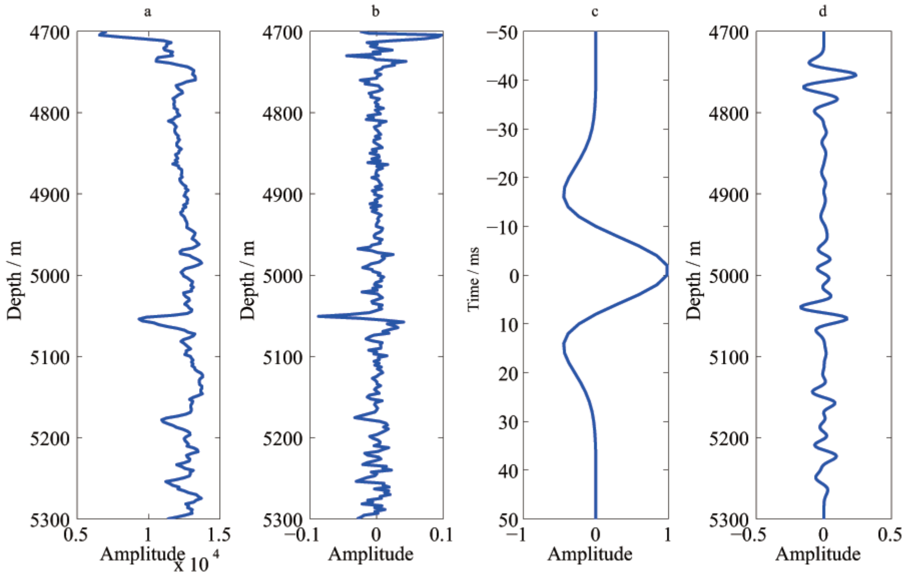

Figure 5. Real seismic data of one trace: (a) acoustic impedance of the well with depth 4700 m to 5300 m, (b) reflection coefficient calculated using equation (4.1), (c) Ricker wavelet with center frequency 40 Hz, (d) synthetic seismic trace resulting from the convolution of the reflection coefficient and Ricker wavelet.

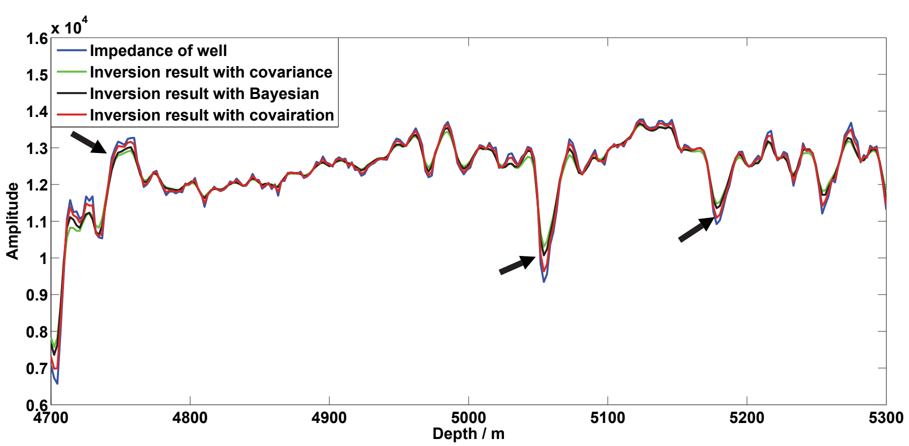

Figure 6. Impedance inversion results of the covariation, covariance and Bayesian methods.

for assessing the quality of the fit. It is seen that the residual is small and the ratio is less than 2.5 %. This analysis shows that the covariation inversion method is effective in the acoustic impedance inversion.

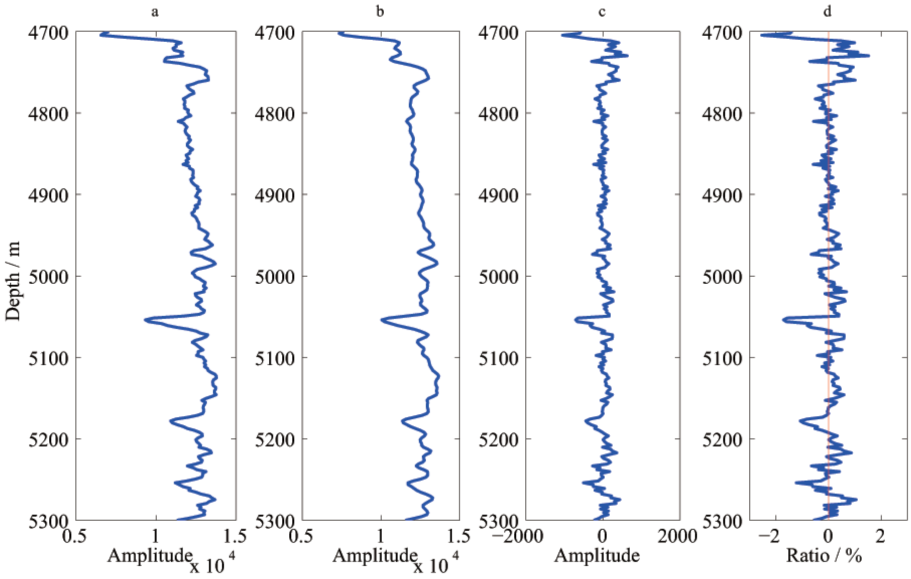

Figure 7. Acoustic impedance inversion result of one trace: (a) acoustic impedance from the well, (b) inversion result when $p = 1.6$, (c) residual of impedance of the well and inversed result, (d) residual ratio.

The prior single trace inversion result showed the feasibility of the proposed covariation method in acoustic impedance inversion. Finally, the inversion process was applied to the entire seismic volume to estimate the Earth's acoustic impedance. The original seismic section of this survey is shown in Figure 8. The inversion calculation was conducted trace by trace with equation (4.8), and the moment is set $p = 1.6$. An inverted acoustic impedance from the target horizon is shown in Figure 9. The acoustic impedance map delivers a clear and reliable structural image of the underground. It is clearly seen that there are some low value clusters near the top, and the clusters may be evaluated as reservoir. According to the well log interpretation result, there is a gas reservoir, marked with red ellipse, at a depth of 4760 m–4783 m (2310 ms–2315 ms). It can be concluded that the inversion result conforms very closely to the well log interpretation, which verifies the correctness of the proposed covariation inversion method.

5 Conclusions

This paper proposed a new covariation acoustic impedance inversion approach based on the non-Gaussian α-stable distribution. Under the assumption that the

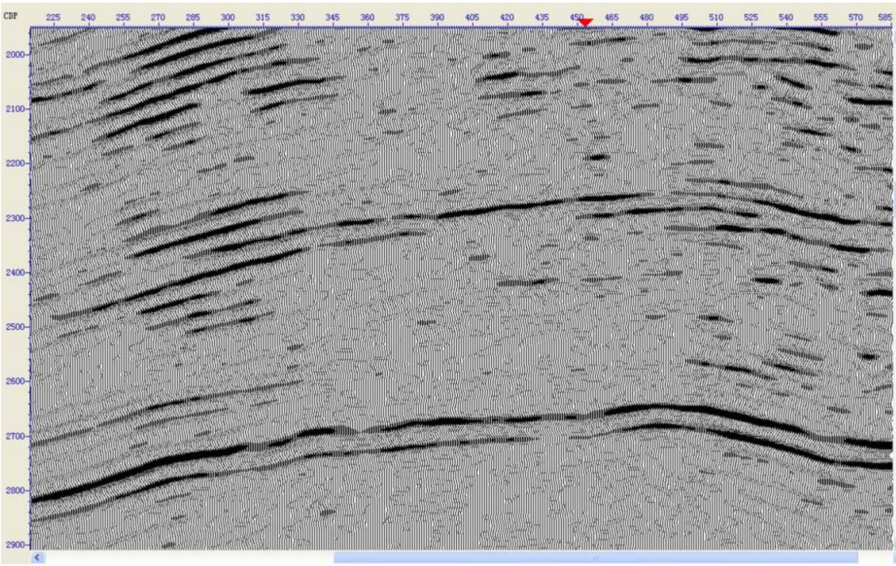

Figure 8. Seismic section.

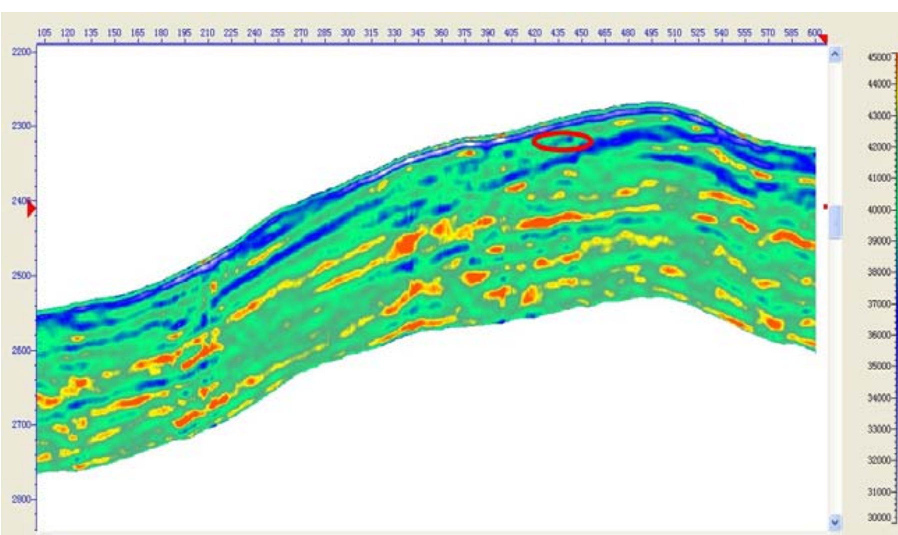

Figure 9. Acoustic impedance inversion with covariation approach.

seismic signals follow non-Gaussian $\boldsymbol{\alpha}$-stable distribution. Consequently, only moments of order less than the characteristic exponent α are finite, and the inversion should be conducted with covariation rather than covariance.

Testing using synthetic data and real seismic data are conducted to verify the performance of the proposed method. In the synthetic data inversion experiment, the synthetic trace is computed as convolution results of a pseudo-reflectivity coefficient with a Ricker wavelet, and the pseudo-reflectivity coefficient is a sparse series. Applying the covariation inversion approach, the inversed result conforms very close to the pseudo-reflectivity coefficient especially at the spikes. In the real seismic data inversion case, the results of both signal trace and whole survey conform closely to the well log interpretation very well. It is important to note that a seismic trace from the nearby well is used to estimate the characteristic exponent via the sample quantile method. Moreover, the moment p of the whole survey is set to be less than the estimated characteristic exponent. The results verify the correctness and effectiveness of the proposed method.

Bibliography

[1] C. R. Conti, M. Roisenberg, G. Neto and M. J. Posani, Fast seismic inversion methods using ant colony optimization algorithm, *IEEE Geosci. Remote Sensing Lett.* **10** (2013), no. 5, 1119–1123.

[2] E. F. Fame and R. Roll, Parameter estimation for symmetric stable distributions, *J. Amer. Statist. Assoc.* **66** (1971), 331–338.

[3] Y. Gao, T. S. Qiu and Y. L. Zhang, A novel multi-source time delay estimation method based on CTZ and covariation spectrum, *J. Dalian Univ. Technol.* **47** (2007), no. 5, 746–750.

[4] R. Godfrey and J. F. Claerbout, Two methods of deconvolution: Power spectrum smoothing and parsimonious deconvolution, *Stanford Exploration Project* **14** (1978), 207–225.

[5] J. Gunning and M. E. Glinskey, Delivery: An open-source model-based Bayesian seismic inversion program, *Comput. Geosci.* **30** (2004), no. 6, 619–639.

[6] E. P. Leite and A. C. Vidal, 3D porosity prediction from seismic inversion and neural networks, *Comput. Geosci.* **37** (2011), no. 8, 1174–1180.

[7] T. H. Liu and J. M. Mendel, A subspace-based direction finding algorithm using fractional lower order statistics, *IEEE Trans. Signal Process.* **49** (2001), no. 8, 1605–1613.

[8] W. H. Liu, Y. Y. Wang and T. S. Qiu, Evoked potential latency delay estimation by using covariation correlation approach, in: *The 2nd International Conference on Bioinformatics and Biomedical Engineering – ICBBE 2008* (Shanghai 2008), IEEE Press, New York (2008), 652–655.

[9] X. Y. Ma and C. L. Nikias, Parameter estimation and blind channel identification in impulsive signal environments, *IEEE Trans. Signal Process.* **43** (1995), no. 12, 2884–2897.

[10] J. H. McCulloch, Simple consistent estimators of stable distribution parameters, *Comm. Statist. Simulation Comput.* **15** (1986), no. 4, 1109–1136.

[11] C. L. Nikias and M. Shao, *Signal Processing with Alpha-Stable Distributions and Application*, John Wiley and Sons, New York, 1995.

[12] M. Shao and C. L. Nikias, Signal processing with fractional lower order moments: Stable processes and their applications, *Proc. IEEE* **81** (1993), no. 7, 986–1010.

[13] R. P. Srivastava and M. K. Sen, Fractal-based stochastic inversion of poststack seismic data using very fast simulated annealing, *J. Geophys. Eng.* **6** (2009), no. 4, 412–425.

[14] P. Tsaklides and C. L. Nikias, The robust covariation-based MUSIC (ROC-MUSIC) algorithm for bearing estimation in impulsive noise environment, *IEEE Trans. Signal Process.* **44** (1996), no. 7, 1623–1633.

[15] A. T. Walden, Non-Gaussian reflectivity, entropy, and deconvolution, *Geophysics* **50** (1985), 2862–2888.

[16] J. Wang, E. E. Kuruoglu and T. Zhou, Alpha-stable channel capacity, *IEEE Comm. Lett.* **15** (2011), no. 10, 1107–1109.

[17] S. Y. Wang and X. B. Zhu, α-spectrum estimation method for ARMA process based on FLOC, *J. Commun.* **28** (2007), no. 7, 98–103.

[18] L. Q. Yang, H. B. Song and T. Y. Hao, Application of impedance inversion based on BP neural network, *Progr. Geophys.* **20** (2005), no. 1, 34–37.

[19] B. B. Yue, Z. M. Peng, Y. G. Hong and and W. Zou, Wavelet inversion of pre-stack seismic angle-gather based on particle swarm optimization algorithm, *Chinese J. Geophys.* **52** (2009), no. 12, 3116–3123.

[20] B. B. Yue, Z. M. Peng and Q. H. Zhang, Seismic inversion method with α-stable distribution, *Chinese J. Geophys.* **55** (2012), no. 4, 1307–1317.

Received October 14, 2013.

Author information

Bi B. Yue, No. 4, Section 2, North Jianshe Road, 610054 Chengdu, P. R. China.
E-mail: yuebibo@gmail.com

Zhen M. Peng, No. 4, Section 2, North Jianshe Road, 610054 Chengdu, P. R. China.
E-mail: zmpeng@uestc.edu.cn